

Magnetic dipole probes of the sd and pf shell crossing in the $^{36,38}\text{Ar}$ isotopes \star

A. F. Lisetskiy^aE. Caurier^b K. Langanke^{a,c}
 G. Martínez-Pinedo^a P. von Neumann-Cosel^c F. Nowacki^b
 A. Richter^c

^a*GSI, Planckstr.1, D-64291, Darmstadt, Germany*

^b*Institut de Recherches Subatomiques, Université Louis Pasteur, 67037 Strasbourg, France*

^c*Institut für Kernphysik, Technische Universität Darmstadt, D-64289, Darmstadt, Germany*

Abstract

We have calculated the M1 strength distributions in the $^{36,38}\text{Ar}$ isotopes within large-scale shell model studies which consider valence nucleons in the sd and pf shells. While the M1 strength in ^{36}Ar is well reproduced within the sd shell, the experimentally observed strong fragmentation of the M1 strength in ^{38}Ar requires configuration mixing between the sd and the pf shells adding to our understanding of correlations across the $N=20$ shell gap.

Key words:

Large Scale Shell Model, B(M1), spin-flip

PACS: 21.10.Ft; 21.60.Cs; 21.60.-n;

1 Introduction

The shell model concepts of *closures*, *magic numbers* and *inert cores* leads to a reasonably good description of nuclear phenomena in light as well as in heavy nuclei. However, recent experimental findings show that shell closures might get eroded in very neutron-rich nuclei and that the inter-shell correlations

\star This work has been supported through the SFB634 of the Deutsche Forschungsgemeinschaft.

Email address: olisetsk@theory.gsi.de (A. F. Lisetskiy).

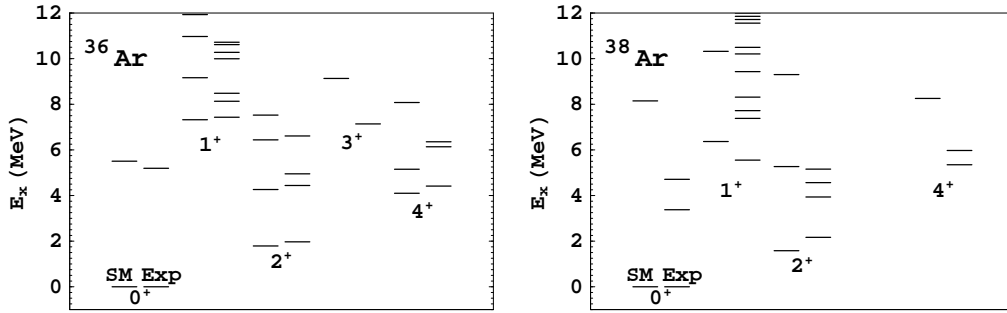


Fig. 1. Calculated and experimental spectra for ^{36}Ar (left) and ^{38}Ar (right). Excitation energy E_x is plotted along the y-axis. The calculations have been performed in the sd shell using the USD interaction [3]. The model space allows only the formation of positive parity states.

among nucleons play a decisive role for the structure of these nuclei. A famous example is the nucleus ^{32}Mg which is strongly deformed in the ground state, despite its neutron number $N = 20$, e.g. [1]. Thus, shell closures are not 'rigid' and there have been for a long time indications for cross-shell correlations even in nuclei close to classical double-magic nuclei like ^{40}Ca . For this nucleus, these include the observation of a strong M1 transition [2] and of a non-vanishing Gamow-Teller (GT) strength built on the ^{40}Ca ground state [4,5,6]. On the theory side, recent studies [7,8] show that there are very large admixtures of sd configurations in low-energy states of Ca isotopes with $A \geq 40$, although these nuclei are usually considered as "good" pf shell nuclei. Another indication for the erosion of the sd - pf closure near $A = 40$ are the data for the M1 strength in ^{36}Ar and ^{38}Ar [9]. While experimentally the M1 strength distribution for both nuclei is rather fragmented, this feature is reproduced by sd shell model calculations for ^{36}Ar , while these studies predict only one strong M1 transition for ^{38}Ar , in clear contradiction to the data [9]. Obviously a single sd -shell model space, allowing only for two proton holes with respect to a ^{40}Ca core, besides a closed neutron shell, is too limited for a description of the M1 data in ^{38}Ar .

The fact that cross-shell excitations are quite important is revealed by a detailed comparison of the experimental and calculated spectrum at low energies. The shell model calculations have been performed within the sd shell using the standard USD interaction [3]. The model space does not allow the formation of negative parity states, but the calculation also misses a few of the low-lying 0^+ and 2^+ states in ^{38}Ar , while the agreement between theory and experiment is quite sufficient for the positive parity states in ^{36}Ar (see Fig.1). In Fig.2 we compare the experimental M1 strength distribution with the shell model results, which are similar to those published earlier in [9]. The shell model code ANTOINE [10] has been used for all calculations presented in this paper.

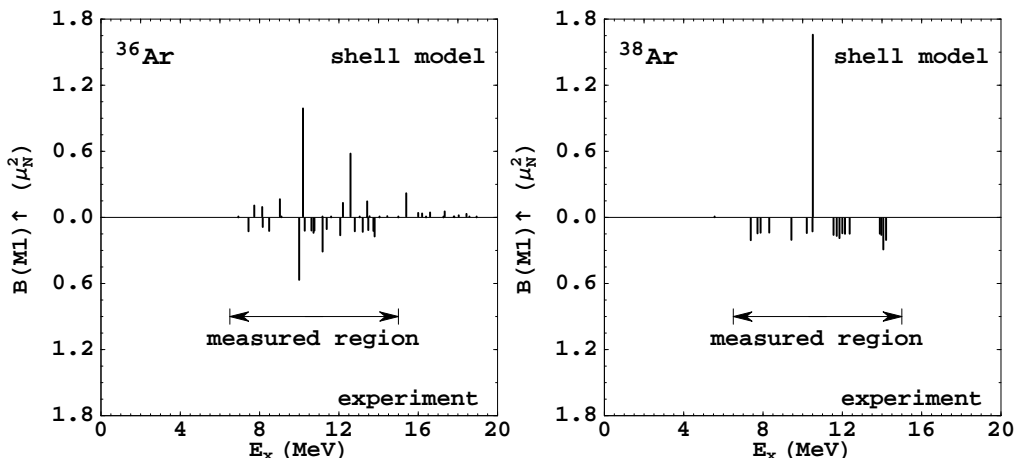


Fig. 2. Calculated and experimental M1 $0_1^+ \rightarrow 1_f^+$ strength distributions for ^{36}Ar (left) and ^{38}Ar (right). The calculations have been performed in the sd -shell using the USD interaction [3]. The spin part of the M1 operator has been quenched by a factor of 0.75 which is in agreement with the one deduced for other nuclei in this mass range [11]. The same quenching of the spin part of the M1 operator has been used throughout this paper. Experimental error bars, which are of order of 10% for all measured states, are not shown here and in all further figures.

The detailed comparison of the sd -shell model results with the data shows that the M1 data for the two argon isotopes ^{36}Ar and ^{38}Ar present a challenge to theory: correlations between sd and pf shells should not affect the major features of the M1 strength distribution for ^{36}Ar , but must be essential for the ^{38}Ar M1 data, e.g. if only two neutrons are added to the nucleus.

The present paper is an attempt to reproduce this striking behavior on the basis of large-scale shell model calculations which combine both sd and pf shells. We have followed two routes. At first, we have performed studies within the complete $sdpf$ shell. However, due to computational limitations these calculations had to be restricted to 2-particle 2-hole (2p2h) and 4p4h excitations from the sd - to the pf -shell. These studies were supplemented by full diagonalization calculations within the $d_{3/2}s_{1/2}f_{7/2}p_{3/2}$ model space (denoted as $sdpf_0$ space below). Further additional 1p1h coupling between the $d_{5/2}$, $f_{5/2}$, $p_{1/2}$ orbitals and the $sdpf_0$ space has been taken into account – this extended space is referred to as $sdpf_1$ below. As we will show in the following sections, the calculations in the $sdpf_1$ model space indeed result in fragmentation of the M1 strength for both argon isotopes and also reproduce their low-energy excitation spectrum.

2 Truncated shell model studies in the complete $sdpf$ shells

There have been several attempts to derive a suitable effective interaction for the $sdpf$ model space (see, for example [12,13,14] and references therein). For our study we adopt the one of Ref. [14]. This interaction contains three parts: the USD interaction for the sd -shell [3], the KB' matrix elements for the pf shell [15] and the G-matrix of Kahana, Lee and Scott for the cross-shell matrix elements [16]. The $f_{7/2}d_{3/2}$, $f_{7/2}s_{1/2}$, $p_{3/2}s_{1/2}$ and $p_{3/2}d_{3/2}$ monopole terms have been adjusted to some recent experimental data [14]. We note that there is a problem with spurious center-of-mass (COM) excitations for the chosen configuration space. To treat this problem we have added the tenfold of the center-of-mass Hamiltonian to the original Hamiltonian [14]. This procedure pushes states with predominantly center-of-mass excitations up in energy and practically eliminates the spurious excitations in the low-energy states of interest here.

Unfortunately full diagonalization studies are yet not possible in the complete $sdpf$ model space due to computational limitations. However, it is feasible to perform calculations for ^{38}Ar in which 2 particles or even 4 particles are promoted from the sd shell to the pf shell. We will refer to these studies as 2p2h and 4p4h calculations, respectively. The dimension of the 4p4h model space is 227 625 436 for $M = 0^+$ states in the m-coupling scheme. For ^{36}Ar we have performed 2p2h calculations, corresponding to 3 148 356 $M = 0^+$ states.

These studies, however, showed no improvement for the ^{38}Ar spectrum compared to the pure sd -shell results. In fact the first excited 0^+ state lies at an excitation energy above 7 MeV, with very little mixing to the ground state which had basically an sd shell configuration. Consequently no fragmentation has been found in our calculation of the M1 strength distributions for ^{38}Ar . We also have performed No-Core Shell Model [17,18] calculations in a $4\hbar\omega$ model space using the UCOM interaction [19] obtaining similar results.

The mixing of the sd and pf shell configurations can be enhanced by slight monopole modifications in the interaction. This strategy has been applied in large-scale shell model calculations of ^{36}Ar and leads to a quite satisfying description of the strongly deformed 4p4h band and its coupling to the ground state band [20]. Following this reference we have lowered the energy of the $npnh$ configurations with $n = 4$ and $n = 6$ by suitable monopole shifts, in this way enforcing pf -shell configurations to mix into the ground states. As it is expected the mixing results in fragmentation of the M1 strength distribution. This can be seen in Fig.3 which shows the calculated M1 strength for ^{38}Ar obtained in a 4p4h calculation and employing Lanczos diagonalization with 50 iterations. Indeed the strong M1 transition observed in the pure sd -shell calculation is now split into several components and some M1

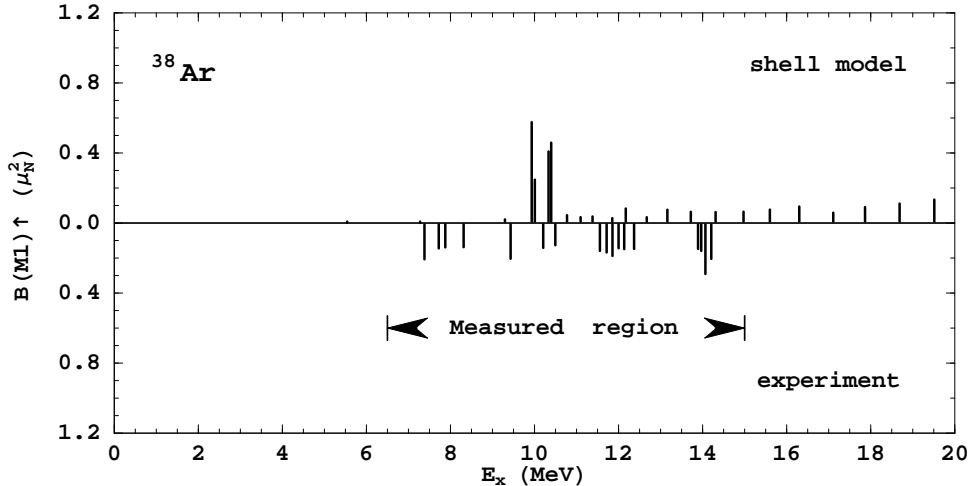


Fig. 3. Calculated (upper panel) and experimental (lower panel) M1 strength distributions in ^{38}Ar in the full $sdpf$ space with 4p4h cross-shell excitations. The calculations have been performed using a monopole-modified interaction as described in the text.

strength is shifted to higher excitation energies. Nevertheless, the agreement with data is only marginal. In particular, the data show already some M1 strength around 8 MeV, which is missing in the calculation. This is possibly improved if nph configurations with $n > 4$ were included – previous shell model studies [7,8,13,14] indicated that energies of the states in nuclei around ^{40}Ca are converging rather slowly when nph cross-shell excitations with larger n are gradually added. While such converged calculations are yet impossible in the complete $sdpf$ shell, they are, however, feasible in the $sdpf_0$ and $sdpf_1$ model spaces (see text above) to which we turn in the next section.

3 Large-scale shell-model calculations in the truncated $sdpf$ model space

We have performed diagonalization calculations in the $sdpf_1$ model space which includes the spin-orbit partners (missing in the $sdpf_0$ space) approximately by allowing 1p1h excitations from the $d_{5/2}$ orbital to the rest of the sd shell, and from the $f_{7/2}p_{3/2}$ space to the $f_{5/2}p_{1/2}$ sub-space, respectively. In other words we put 1p1h predominantly spin-flip excitations on top of the complex nph $(s_{1/2}d_{3/2})^{A-28-n}(f_{7/2}p_{3/2})^n$ cross-shell configurations obtained within the $sdpf_0$ space. This extension increases the dimension of the model space from 2.3 million ($sdpf_0$) to nearly 75 million ($sdpf_1$) for ^{38}Ar . For the calculations we have used the same effective interaction as in [7]. The $sdpf_0$ model space allows up to 8 or 10 particles to be promoted from the sd -shell to the pf -shell for ^{36}Ar and ^{38}Ar , respectively. It turns out these cross-shell

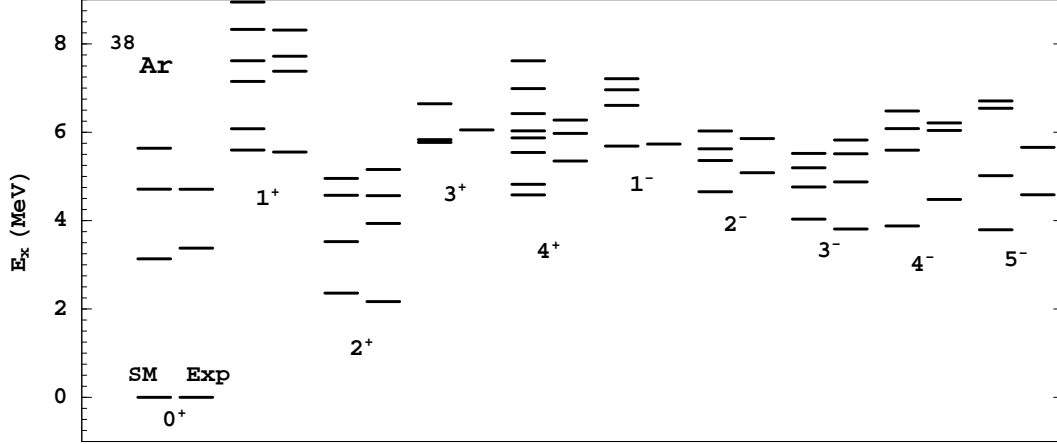


Fig. 4. Calculated and experimental spectra for ^{38}Ar within the full $sdpf_1$ space.

excitations are sufficient to achieve a good agreement between our calculations and the experimental ^{38}Ar spectrum. As one can observe in Fig. 4, the calculation now yields the low-lying 0^+ and 2^+ excitations which were missing in the sd -model space (see Fig. 1). The calculated ^{36}Ar spectrum in the $sdpf_1$ model space (see Fig. 5) agrees similarly well with the data as the pure sd -shell result (Fig. 1) for the positive parity states. For both argon isotopes the calculated negative parity spectrum, missing in the pure sd -shell studies, agrees quite well with the observed one.

It is interesting to inspect more closely the role of $n\nu nh$ cross-shell and $1\nu 1h$ spin-flip excitations in the $sdpf_1$ space for the ^{36}Ar and ^{38}Ar ground states. To quantify the importance of $n\nu nh$ cross-shell excitations we have calculated

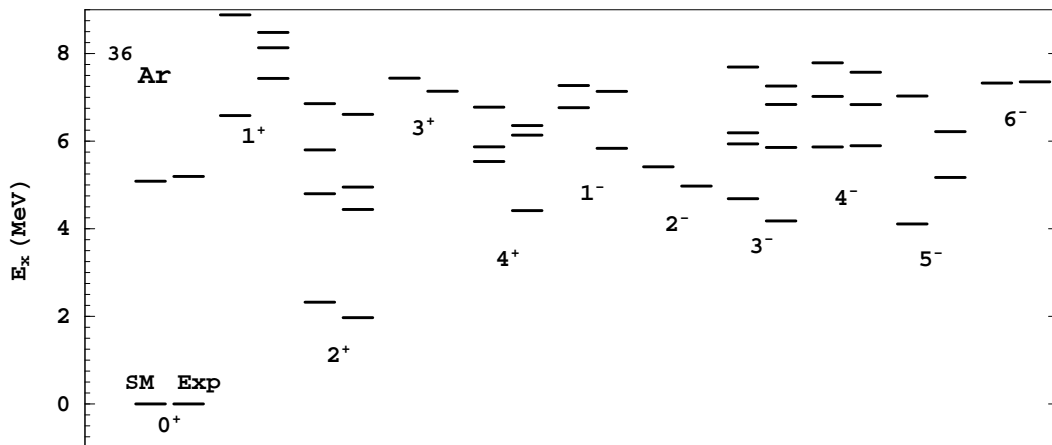


Fig. 5. Calculated and experimental spectra for ^{36}Ar within the full $sdpf_1$ space.

Table 1

The structure of the ground state and of two final states with strong M1 transitions (the $1^+, T = 1$ at 10.14 MeV and the $1^+, T = 1$ at 14.77 MeV states) for ^{36}Ar in the full $sdpf_1$ space. The coefficient $A_n(n_{df})$ gives the contribution of the component with n particles promoted across the sd - pf shell gap. The n_{df} quantity indicates whether 1p1h spin-flip components are present ($n_{df} = 1$) or not ($n_{df} = 0$). Only components with weights larger than 0.01 are shown.

$J_i^\pi = 0_1^+, T = 0$			
n	0	2	4
$A_n(0)$	0.47	0.30	0.05
$A_n(1)$	0.01	0.11	0.04
$J_i^\pi = 1^+, T = 1$ ($E_x = 10.14$ MeV)			
n	0	2	4
$A_n(0)$	0.14	0.51	0.08
$A_n(1)$	0.03	0.13	0.09
$J_i^\pi = 1^+, T = 1$ ($E_x = 14.77$ MeV)			
n	0	2	4
$A_n(0)$	0.02	0.38	0.15
$A_n(1)$	0.07	0.23	0.14

the weights $A_n(n_{df} = n_d + n_f)$ of the

$$(d_{5/2})^{6-n_d}(s_{1/2}d_{3/2})^{A-28-n+n_d}(f_{7/2}p_{3/2})^{n-n_f}(f_{5/2}p_{1/2})^{n_f}$$

configurations, where $n_{df} = n_d + n_f$ define the total number of excitations from the $d_{5/2}$ orbital to the rest of the sd -shell and from the $(f_{7/2}p_{3/2})$ subspace to the respective spin-orbit partners. Our calculations are restricted to $n_{df} = 1$. Thus, with $A_n(n_{df} = 1)$ we have identified the components of the wave functions which arise from 1p1h couplings to the spin-orbit partners within the sd -shell ($n_d = 1, n_f = 0$) or pf -shell ($n_d = 0, n_f = 1$), respectively. The dominant configurations of the ground state wave functions are given in Tables 1 and 2 for ^{36}Ar and ^{38}Ar , respectively. In the $sdpf_1$ model space, approximately half of the ^{36}Ar ground state corresponds to pure sd -shell configurations, where the 1p1h excitations of the $d_{5/2}$ orbit play a tiny role (1%).

Cross-shell 2p2h components contribute about 41% to the ^{36}Ar ground state, where the couplings to the spin-orbit partners are now sizable (11%). Higher-order cross-shell components with $n > 2$ are relatively unimportant (less than 10%). These components, however, are larger in the ^{38}Ar ground state. We find that this state is dominated by n pnh cross-shell excitations with $n \leq 4$, with 0p0h and 2p2h excitations amounting to about 75% of the wave function.

Table 2

The structure of the ground state ($0^+, T = 1$) and of two final states with sizable M1 transitions (the $1^+, T = 1$ at 12.96 MeV and the $1^+, T = 2$ at 18.22 MeV states) for ^{38}Ar in the full $sdpf_1$ space. The coefficient $A_n(n_{df})$ gives the contribution of the component with n particles promoted across the sd - pf shell gap. The n_{df} quantity indicates whether 1p1h spin-flip components are present ($n_{df} = 1$) or not ($n_{df} = 0$). Only components with weights larger than 0.01 are shown.

$J_i^\pi = 0_1^+, T = 1$				
n	0	2	4	6
$A_n(0)$	0.33	0.34	0.13	0.02
$A_n(1)$	0.0	0.09	0.07	0.01
$J_i^\pi = 1^+, T = 1 (E_x = 12.96 \text{ MeV})$				
n	0	2	4	6
$A_n(0)$	0.0	0.15	0.30	0.09
$A_n(1)$	0.05	0.13	0.19	0.08
$J_i^\pi = 1^+, T = 2 (E_x = 18.22 \text{ MeV})$				
n	0	2	4	6
$A_n(0)$	0.0	0.04	0.27	0.12
$A_n(1)$	0.0	0.11	0.29	0.16

Importantly, the pure sd -shell configuration contributes only 33% to the ^{38}Ar ground state. The rest corresponds to excitations to the pf shell and hence opens new channels for the fragmentation of the M1 strength distribution, to which we turn now.

We have calculated the M1 strength distributions by using the Lanczos method with 200 iterations. This is sufficient to achieve convergence for the calculated energies of the lowest states. However, at higher excitation energies the calculated M1 distributions represent only the total strength per energy interval rather than true states. We note that we have scaled the spin part of the M1 operator by a constant factor $q = 0.75$, as it is customary in shell model calculations. It has been shown that shell model calculations using such an effective spin operator describe the M1 [11] and GT [21,22] transitions of pf -nuclei quite well.

The calculated M1 strength distributions for ^{36}Ar and ^{38}Ar within the full $sdpf_1$ model space are shown in Fig.6. For ^{36}Ar the result is similar to the sd -shell calculation as, in agreement with the experimental data, it shows a rather strong transition at around 10 MeV. At higher energies, the present ^{36}Ar M1 strength distribution is significantly more fragmented than the one

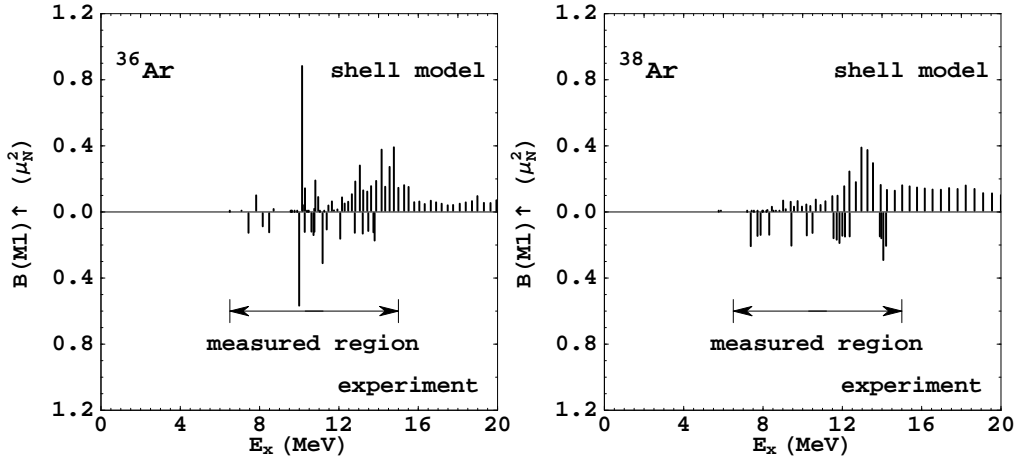


Fig. 6. Comparison of the experimental and theoretical M1 strength distributions for ^{36}Ar (left) and ^{38}Ar (right) calculated in the $sdpf_1$ model space.

obtained within the pure sd -shell. Our calculation also predicts a noticeable amount of M1 strength outside of the experimental energy window. In fact, we calculate a total M1 strength for ^{36}Ar of $6.76 \mu_N^2$. Experimentally a summed M1 strength of $2.65(12) \mu_N^2$ is observed up to an excitation energy of 13.8 MeV, which is in agreement with the calculated value ($2.8 \mu_N^2$). However, our calculation predicts an M1 strength of $1.4 \mu_N^2$ in the energy interval 13.8-15 MeV, where experimentally no strength has been observed.

For ^{38}Ar the result from the $sdpf_1$ model space is strikingly different than that of the pure sd -shell calculation reported above. The calculated M1 strength in the energy regime below 15 MeV is now strongly fragmented like the experimental one. Moreover, we find a total M1 strength of $2.88 \mu_N^2$ in the experimental energy window, to be compared with the experimental value of $2.86(18) \mu_N^2$. For ^{38}Ar (with a $T = 1$ ground state) M1 transition can lead to final states with $T = 1$ and $T = 2$. Most of the M1 strength to $T = 2$ states resides at excitation energies above 15 MeV so that the main peak of the M1 strength distribution around $E_x = 13$ MeV corresponds dominantly to $\Delta T = 0$ transitions. As for ^{36}Ar , our calculation predicts a strong part of the M1 strength to reside at energies higher than the current experimental energy window. In fact, our calculated total M1 strength is $6.01 \mu_N^2$ for ^{38}Ar . It would be desirable to experimentally search for this predicted M1 strength at higher energies.

To explore the origin of the fragmentation observed in the M1 distributions for both argon isotopes, we have also analyzed the wave functions of the strongest 1^+ states.

For ^{36}Ar , Table 1 lists the dominant configurations of the $1^+, T = 1$ state at

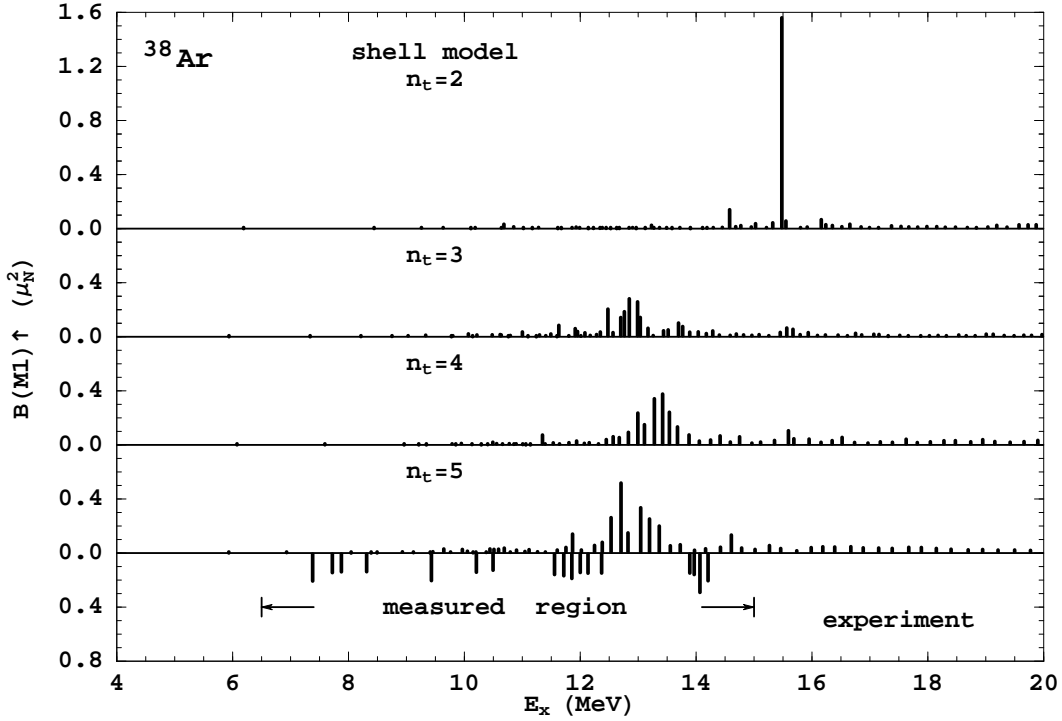


Fig. 7. Evolution of the M1 strength distribution with increase of the model space. Here $n_t = n + n_{df}$, where n is the number of particles excited across the sd - pf gap and $n_{df} \leq 1$ stands for the number of nucleons promoted from the $d_{5/2}$ orbital to the $s_{1/2}d_{3/2}$ subspace and from the $f_{7/2}p_{3/2}$ to the $f_{5/2}p_{1/2}$ ones.

10.14 MeV, which corresponds to the single strong M1 transition observed in the calculation (and in the data), and the 1^+ , $T = 1$ state at 14.77 MeV, which is a typical state in the energy range of strongly fragmented M1 transitions. The 1^+ state at 10.14 MeV is dominated by $0p0h$ and $2p2h$ configurations ($> 80\%$), similarly to the ground state. We notice that the state has a quite significant $2p2h$ component (40%) with a simultaneous cross-shell excitation of a proton and a neutron. Thus, we find, as in the pure sd -shell calculations, a strong M1 transition around 10 MeV, however, the configurations of the initial and final states are quite different in the sd and the $sdpf_1$ model spaces. The 1^+ state at 14.77 MeV has sizable $4p4h$ configurations (about 30%), but in contrast it has a rather small $0p0h$ component (less than 10%). In this energy range the various configurations are quite strongly mixed resulting in the strong fragmentation of the M1 strength.

For ^{38}Ar Table 2 lists the dominant configurations of the 1^+ , $T = 1$ state at 12.96 MeV which carries a sizable fraction of the fragmented M1 strength below 15 MeV. Different to the ground state, $0p0h$ excitations (pure sd -shell configurations) amount only to 5%, while $2p2h$ and $4p4h$ excitations are dominant. But importantly we also find a noticeable contribution of $6p6h$ configurations in these states. It is further worth mentioning that neutron excitations

are more important than proton excitations.

Obviously there are many 1^+ states with large configuration mixing at moderate excitation energies which have a substantial pf -shell contribution, but only a rather small pure sd -shell component or a nearly vanishing $0p0h$ component. Table 2 lists the dominant configurations of the $1^+, T = 2$ state at 18.22 MeV, which is a typical example in this energy regime.

Finally we have explored the evolution of the M1 strength distribution in ^{38}Ar with the number of allowed cross-shell excitations. It is convenient to characterize the different truncations using the quantity $n_t = n + n_{df}$, where n is the number of particles moved across the sd - pf shell gap and n_{df} indicates the number of nucleons moved from the $d_{5/2}$ orbital to the $s_{1/2}d_{3/2}$ subspace and from the $f_{7/2}p_{3/2}$ subspace to the spin-orbit partners $f_{5/2}p_{1/2}$. In our $sdpf_1$ calculations we have allowed only $1p1h$ excitations between spin-orbit partners, hence $n_{df} \leq 1$. The simplest excitation scheme is $n_t = 2$ which allows the mixing of three configurations, namely the one with $n = 0, n_{df} = 0$, $n = 2, n_{df} = 0$ and $n = 0, n_{df} = 1$. (Note that $n = 1$ excitations are not possible due to parity.) The $n_t = 2$ excitations do not change qualitatively the shape of the M1 strength function (see Fig. 7) as compared to the pure sd -shell results. Only the centroid is moved to higher energies, as the original single spin-flip state is shifted up in energy and is connected by the M1 operator only to the $n = 0, n_{df} = 0$ configuration. If the number of excitations is increased to $n_t = 3$, only one new configuration with $n = 2, n_{df} = 1$ is added. This configuration is, however, crucial for the fragmentation of the M1 strength (see Fig. 7). Besides the large M1 matrix element between the $n = 0, n_{df} = 0$ and $n = 0, n_{df} = 1$ configurations in the sd -shell, there is now another big M1 transition in the model space (between the $n = 2, n_{df} = 0$ and $n = 2, n_{df} = 1$ configurations) involving $2p2h$ excitations across the shell gap. The interference of these two contributions produces the fragmentation of the M1 strength. The further addition of new components like $n = 4, n_{df} = 0$ ($n_t = 4$) and $n = 4, n_{df} = 1$ ($n_t = 5$) does not change the fragmentation picture qualitatively, however, the summed $B(M1)$ strength increases from $2.95 \mu_N^2$ ($n_t = 3$ case) to $4.02 \mu_N^2$ and $4.20 \mu_N^2$, respectively, as more pf -shell components are mixed into the ground state wave function. We also observe that the convergence for the energies of many states is not even achieved at the $n_t = 5$ level (see Fig. 8). This indicates that more complicated configurations with $n_t > 5$ have to be included, which we have done in our complete $n = 10, n_{df} = 1$ ($n_t = 11$) calculation discussed above.

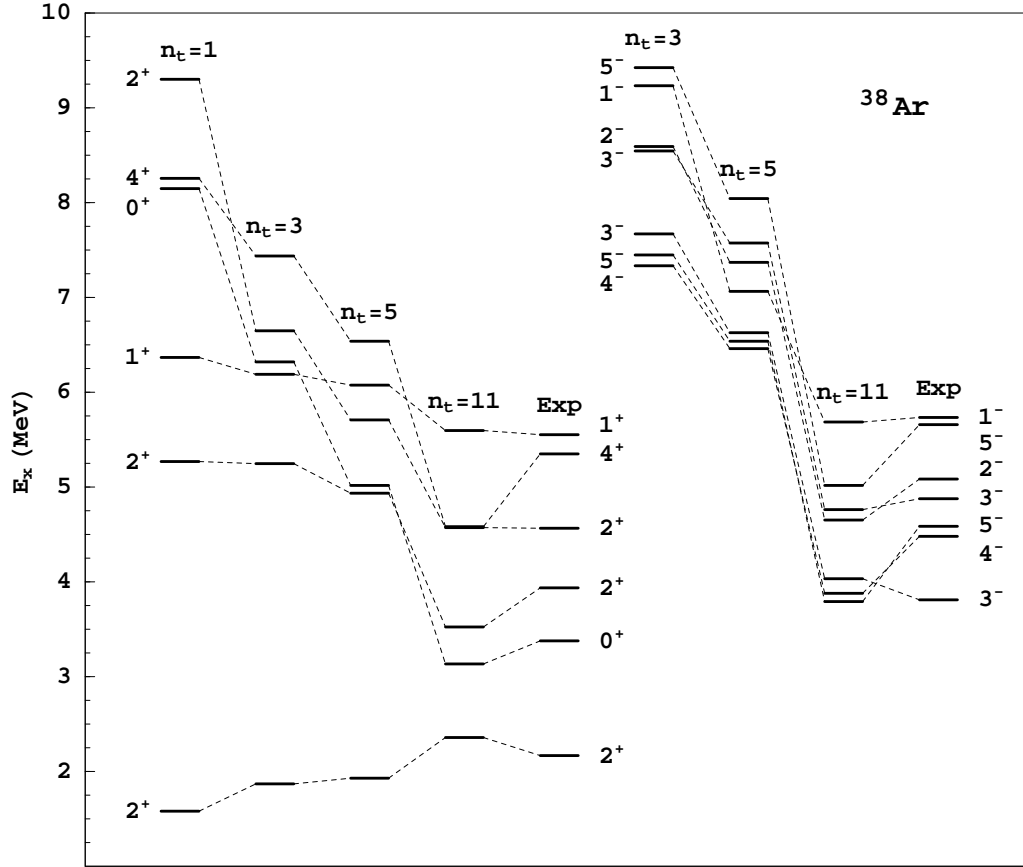


Fig. 8. Comparison of experimental and calculated spectra for ^{38}Ar in the $sdpf_1$ space for different values of $n_t = n + n_{df}$ with n_{df} fixed at 1 and varying n corresponding to n pnh cross-shell excitations. The full $sdpf_1$ space calculation corresponds to $n_t = 11$.

4 Conclusion

We have performed large-scale shell model calculations for ^{36}Ar and ^{38}Ar within the complete $s_{1/2}d_{3/2}f_{7/2}p_{3/2}$ model space and additionally allowing 1p1h excitations from $d_{5/2}$ to the $s_{1/2}$, $d_{3/2}$ orbitals or from $f_{7/2}$ and $p_{3/2}$ to the rest of the pf -shell. We reproduce the energy spectra for both isotopes, including the negative parity states. Importantly our calculations identify sizable contributions of cross-shell components in the ^{36}Ar and ^{38}Ar ground states, implying the onset of erosion of the $N=20$ shell closure. However, this erosion is a slow process involving many n pnh excitations until, for example, convergence of the energies of the lowest excited states is achieved. These studies reveal the onset of fragmentation in the M1 strength distributions. However, only a marginal agreement with the data has been obtained, which might be improved if higher-order cross-shell excitations are considered.

These cross-shell excitations play an important role for the M1 strength distributions. For ^{36}Ar our calculation exhibits a single strong M1 transition at 10 MeV, which is in agreement with the measured distribution. At higher excitation energies the calculated distribution is quite strongly fragmented, in contrast to the results of pure *sd*-shell calculations. Most of this fragmented strength resides, however, outside of the energy range for which currently data exist.

For ^{38}Ar our calculated M1 distribution is in even stronger contrast to the one obtained in the pure *sd*-shell. The cross-shell *n**p**n**h* excitations lead to a very strong fragmentation of the strength. Particularly important are here $(s_{1/2}d_{3/2})^{10-n}(f_{7/2}p_{3/2})^n$ configurations with $n = 2, 4$ and 6 which are strongly mixed in the wave functions of 1^+ states above 10 MeV. Consequently, also the configurations which include 1*p*1*h* spin-flip excitations involving the $d_{5/2}$, $f_{5/2}$ and $p_{1/2}$ partners build on top of the *n**p**n**h* cross-shell excitations get strongly mixed as well. As a consequence the M1 strength distribution is strongly fragmented, as observed in the data. As for ^{36}Ar our calculation predicts also for ^{38}Ar a sizable amount of M1 strength to reside at energies higher than the current observational limit.

Very recent experimental data [24] obtained via the $^{40}\text{Ar}(\vec{\gamma}, \gamma')$ photon scattering reaction suggest a very strong fragmentation of the M1 strength in ^{40}Ar , where only one 1^+ state with a $B(\text{M1})$ value of $0.145(59) \mu_N^2$ has been identified in the energy region between 7.7 and 11 MeV. The evolution of the M1 strength with increase of the neutron number ($N > 20$) for Ar isotopes is an intriguing issue which will contribute further to our understanding of the $N = 20$ cross-shell dynamics.

References

- [1] T. Motobayashi, Y. Ikeda, Y. Ando, K. Ieki, M. Inoue, N. Iwasa, T. Kikuchi, M. Kurokawa, S. Moriya, S. Ogawa, H. Murakami, S. Shimoura, Y. Yanagisawa, T. Nakamura, Y. Watanabe, M. Ishihara, T. Teranishi, H. Okuno, R. F. Casten, Phys.Lett. B 346 (1995) 9.
- [2] W. Gross, D. Meuer, A. Richter, E. Spamer, O. Titze, and W. Knüpfner, Phys. Lett. B 84 (1979) 296.
- [3] B. A. Brown and B.H. Wildenthal, Annu. Rev. Nucl. Part. Sci 38 (1988) 29.
- [4] T. Chittrakarn, B. D. Anderson, A. R. Baldwin, C. Lebo, R. Madey, and J. W. Watson, and C. C. Foster, Phys. Rev. C 34 (1986) 80.
- [5] C. Gaarde, J. Rapaport, T. N. Taddeucci, C. D. Goodman, C. C. Foster, D. E. Bainum, C. A. Goulding, M. B. Greenfield, D. J. Hören, E. Sugarbaker, Nucl. Phys. A369 (1981) 258.

- [6] B. K. Park, J. Rapaport, J. L. Ullmann, A. G. Ling, D. S. Sorenson, F. P. Brady, J. L. Romero, C. R. Howell, W. Tornow, C. T. Rönqvist, *Phys. Rev. C* 45 (1992) 1791.
- [7] E. Caurier, K. Langanke, G. Martínez-Pinedo, F. Nowacki and P. Vogel, *Phys. Lett. B* 522 (2001) 240.
- [8] S. Schielke, D. Hohn, K. -H. Speidel, O. Kenn, J. Leske, N. Gemein, M. Offer, J. Gerber, P. Maier-Komor, O. Zell, Y. Y. Sharon and L. Zamick, *Phys. Lett. B* 571 (2003) 29.
- [9] C.W. Foltz, D.I. Sober, L.W. Fagg, H.D. Gräf, A. Richter, E. Spamer and B.A.Brown, *Phys. Rev. C* 49 (1994) 1359.
- [10] E. Caurier, computer code ANTOINE, CRN, Strasbourg, 1989; E. Caurier, F. Nowacki, *Acta. Phys. Pol. B* 30 (1999) 705.
- [11] P. von Neumann-Cosel, A. Poves, J. Retamosa, A. Richter, *Phys. Lett. B* 443 (1998) 1.
- [12] E. K. Warburton, D. E. Alburger, J. A. Becker, B. A. Brown, S. Raman, *Phys. Rev. C* 34 (1986) 1031.
- [13] J. Retamosa, E. Caurier, F. Nowacki, and A. Poves, *Phys. Rev. C* 55 (1997) 1266.
- [14] S. Nummela, P. Baumann, E. Caurier, P. Dessagne, A. Jokinen, A. Knipper, G. Le Scornet, C. Miehé, F. Nowacki, M. Oinonen, Z. Radivojevic, M. Ramdhane, G. Walter, and J.Äystö, *Phys. Rev. C* 63 (2001) 044316.
- [15] A. Poves and A. Zuker, *Phys. Rep.* 70 (1981) 4.
- [16] S. Kahana, H.C. Lee, and C.K. Scott, *Phys. Rev.* 180 (1969) 956.
- [17] D. C. Zheng, B. R. Barrett, L. Jaqua, J. P. Vary, and R. J. McCarthy, *Phys. Rev. C* 48 (1993) 1083.
- [18] P. Navratil and B. R. Barrett, *Phys. Rev. C* 54 (1996) 2986.
- [19] R. Roth, private communication.
- [20] E. Caurier, F. Nowacki, A. Poves, *Phys. Rev. Lett.* 95 (2005) 042502.
- [21] G. Marínez-Pinedo, A. Poves, E. Caurier, A. P. Zuker, *Phys. Rev. C* 53 (1996) R2602.
- [22] K. Langanke, D. J. Dean, P. B. Radha, Y. Alhassid, and S. E. Koonin, *Phys. Rev. C* 52, (1995) 718.
- [23] E. K. Warburton, G. T. Garvey and I. S. Towner, *Ann. Phys. (N.Y.)* 57 (1970) 174.
- [24] T. C. Li, N. Pietralla, A. P. Tonchev, M. W. Ahmed, T. Ahn, C. Angell, M. A. Blackston, A. Costin, K. J. Keeter, J. Li, A. Lisetskiy, S. Mikhailov, Y. Parpottas, B. A. Perdue, G. Rainovski, W. Tornow, H. R. Weller, and Y. K. Wu, *Phys. Rev. C* 73 (2006) 054306.